Journal of
*Marine Science
and Engineering*

MDPI

Article

Angle of Arrival Estimator Utilizing the Minimum Number of Omnidirectional Microphones

Jonghoek Kim

System Engineering Department, Sejong University, Seoul 05006, Republic of Korea; jonghoek@sejong.ac.kr

Abstract: In sound signal processing, angle of arrival indicates the direction from which a propagating sound signal arrives at a point where multiple omnidirectional microphones are positioned. Considering a small underwater platform (e.g., underwater unmanned vehicle), this article addresses how to estimate a non-cooperative target's signal direction utilizing the minimum number of omnidirectional microphones. It is desirable to use the minimum number of microphones, since one can reduce the cost and size of the platform by using small number of omnidirectional microphones. Suppose that each microphone measures a real-valued sound signal whose speed and frequency information are not known in advance. Since two microphones cannot determine a unique AOA solution, this study presents how to estimate the angle of arrival using a general configuration composed of three omnidirectional microphones. The effectiveness of the proposed angle of arrival estimator utilizing only three microphones is demonstrated by comparing it with the state-of-the-art estimation algorithm through computer simulations.

Keywords: direction of arrival; phase difference; micro-positioning; bearing measurements; omnidirectional microphone array

Citation: Kim, J. Angle of Arrival Estimator Utilizing the Minimum Number of Omnidirectional Microphones. *J. Mar. Sci. Eng.* **2024**, *12*, 874. https://doi.org/10.3390/jmse12060874

Academic Editor: Weicheng Cui

Received: 17 April 2024
Revised: 10 May 2024
Accepted: 24 May 2024
Published: 24 May 2024

1. Introduction

In underwater environments, electromagnetic signal is easily dissipated; thus, sound is mainly used for underwater target localization. In sound signal processing, angle of arrival (AOA) indicates the direction from which a propagating sound signal arrives at a point where multiple omnidirectional microphones are positioned. Microphones are used to measure a non-cooperative target's signal in a passive manner. It is argued that AOA is desirable, since it does not require active ping generation. Thus, AOA is power-efficient and the non-cooperative target cannot detect the presence of passive microphones.

In underwater environments, sound speed can change according to various environmental effects (e.g., water temperature and salinity) [1]. Moreover, as microphones measure the signal of a non-cooperative target, the target signal frequency may not be known to a microphone.

Thus, this paper considers the case where each omnidirectional microphone measures a real-valued sound signal whose speed and frequency information are not known in advance. The problem is to find the target signal's direction relative to the array position.

Considering a small underwater platform (e.g., underwater unmanned vehicle), this study addresses how to estimate the signal direction utilizing the minimum number of microphones. By integrating the AOA measurements of the target's sound signal, one or more underwater platforms can estimate the target position without being detected by the target [2–6].

It is desirable to use the minimum number of microphones, since one can reduce the cost and size of the platform by using a small number of microphones. Every omnidirectional microphone collects signals uniformly in all directions. Every microphone is connected to every other microphone. Then, readings of all microphones are processed for AOA estimation.

There are many papers on AOA estimation based on signal measurements at multiple microphones. Various AOA estimators (Minimum Variance Distortionless Response (MVDR) beamformer [7–9], Estimation of Signal Parameters via Rotational Invariance Technique (ESPRIT) [10], or MUltiple SIgnal Classification (MUSIC) [11–13]) utilize phase measurements at each microphone for estimating the signal direction.

In the field of array signal processing, the MUSIC estimator is a classical spectrum estimation algorithm. MUSIC [11–13] estimates the autocorrelation matrix utilizing an eigenspace method. MUSIC [11–13] is based on the idea that the signal subspace is orthogonal to the noise subspace. The reference [14] addressed an adaptive beamformer to achieve high performance in the case of low input signal-to-noise ratio (SNR). The reference [15] integrated a MUSIC-based AOA estimation method that applies to both full arrays and sparse arrays. In reference [16], the authors analyzed the MUSIC estimator in the uniform linear array (ULA) and studied various factors which affect the estimation performance. The authors of [17] modified the classic MUSIC to be competent in unknown non-uniform noisy environments. For estimating the AOA of coherent signals in the ULA, MUSIC was modified by reconstructing a noise subspace [18]. In [19], a DOA estimation method based on spatial difference and a modified projection subspace algorithm was proposed for handling serious misalignment in the AOA estimation of multi-path signals under the background of impulse noise. The reference [20] introduced a modified MUSIC estimator to compute the AOA of multiple radio frequency signals, considering an antenna array with an imperfectly calibrated array response. In [21], the authors studied how to optimize parameters of the MUSIC estimator in order to improve the estimation performance.

To the best of our knowledge, every AOA estimator in the literature used more than three microphones. However, it is desirable to reduce the number of microphones, as we consider the cost and size of the platform.

Since two microphones cannot determine a unique AOA solution, this article presents how to estimate the AOA using a general configuration composed of only three microphones. The outperformance of the proposed AOA estimator utilizing only three microphones is demonstrated by comparing it with the MUSIC estimator through computer simulations. One proves that the proposed AOA estimator outperforms the MUSIC estimator considering both estimation accuracy and computation time.

This study is organized as follows. Section 2 introduces the definitions and assumptions. Section 3 introduces the proposed AOA estimator using only three microphones. MATLAB simulations are addressed in Section 4. Section 5 provides the discussion. Conclusions are addressed in Section 6.

2. Definitions and Assumptions

Let $s(*) = \sin(*)$ and $c(*) = \cos(*)$ for notation simplicity. Let $atan2(y, x)$ denote the angle (phase) of $x + jy$. $atan2(y, x)$ exists in the interval $[-\pi, \pi]$. Considering a list, $\mathbf{L}$, $max(\mathbf{L})$ denotes an element with the maximum value in $\mathbf{L}$. Also, $min(\mathbf{L})$ denotes an element with the minimum value in $\mathbf{L}$. For instance, $min([1, 2, 3]) = 1$ and $max([1, 2, 3]) = 3$.

Let $\mathbf{S}_i$ $(i \in \{1, 2, 3\})$ define the 2D coordinates of the i-th microphone. The microphone configuration with three microphones is depicted in Figure 1. In Figure 1, r defines the distance from every microphone to the origin of the frame. For avoiding the phase wrapping case, this paper assumes that r is less than half of the wavelength. In MATLAB simulations, we set r as 0.4 of the wavelength.

This study considers a target which is sufficiently far from the microphones. Let $\mathbf{u}$ define the unit vector from the origin to the target. Let ϕ define the azimuth angle of the target signal, such that $-\pi < \phi \leq \pi$. Here, ϕ is measured from the x-axis of the microphone configuration. See Figure 1. We have

$$\mathbf{u} = (c(\phi), s(\phi))^T. \tag{1}$$

Our problem is to estimate the AOA ϕ based on signal measurements at three microphones. Recall that every microphone is synchronized to every other microphone.

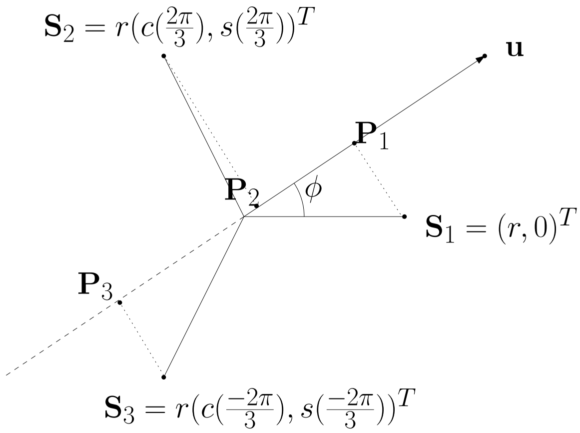

Figure 1. The microphone configuration with three microphones. $\mathbf{u}$ defines the unit vector from the origin to the target. ϕ defines the bearing angle of the target signal, such that $-\pi < \phi \leq \pi$. $\mathbf{S}_i$ $(i \in \{1, 2, 3\})$ defines the 2D coordinates of the i-th microphone. $\mathbf{P}_i$ defines the projection of $\mathbf{S}_i$ onto $\mathbf{u}$.

Let $\mathbf{P}_i$ define the projection of $\mathbf{S}_i$ onto $\mathbf{u}$, as depicted in Figure 1. We have

$$\|\mathbf{P}_i\| = \|\mathbf{S}_i \cdot \mathbf{u}\|. \tag{2}$$

Here, $(\cdot)$ operator indicates the inner product operation, defined as

$$\mathbf{S}_i \cdot \mathbf{u} = \|\mathbf{S}_i\| \|\mathbf{u}\| \cos(a) \tag{3}$$

where a is the angle formed by two vectors $\mathbf{u}$ and $\mathbf{S}_i$. Also, $\|\mathbf{u}\| = 1$, since $\mathbf{u}$ is a unit vector.

Fourier analysis converts a signal from its original time domain to a representation in the frequency domain. DC offset is first removed from the time domain signal at $\mathbf{S}_i$. By applying Fast Fourier Transform (FFT) to the time domain signal, one computes the signal amplitude at different frequencies in the frequency domain. Then, in the frequency domain, one finds a frequency where the signal amplitude is maximized. Let f_i define the frequency where the signal amplitude is maximized.

Let $angle(f_i)$ denote the angle (phase) at f_i $(i \in \{1, 2, 3\})$. Let D_i $(i \in \{1, 2, 3\})$ define the signal delay measurement using the i-th microphone. Using $angle(f_i)$, we can compute the signal delay D_i as

$$D_i = \frac{angle(f_i)}{2\pi f_s}. \tag{4}$$

Here, f_s denotes the sampling frequency.

Let C denote the signal speed. Then, we have

$$D_i = \frac{\mathbf{S}_i \cdot \mathbf{u}}{C}. \tag{5}$$

This implies that in the case where $\mathbf{S}_i \cdot \mathbf{u} > 0$, $D_i > 0$. In addition, in the case where $\mathbf{S}_i \cdot \mathbf{u} < 0$, $D_i < 0$. For instance, in Figure 1, $\mathbf{S}_3 \cdot \mathbf{u} < 0$. Thus, $D_3 < 0$. On the other hand, if $\mathbf{S}_1 \cdot \mathbf{u} > 0$, then $D_1 > 0$.

3. AOA Estimator Using Three Microphones

Before presenting the proposed AOA estimator using three microphones, we show that two microphones cannot determine a unique AOA solution. Suppose that we have only two microphones, $\mathbf{S}_1$ and $\mathbf{S}_2$, as plotted in Figure 2. Then, we draw a straight infinite line connecting these two microphones. In Figure 2, dotted arrows indicate the signal direction at each microphone. Utilizing the phase differences at the two microphones, we cannot determine whether the target exists to the left or to the right of this line. Therefore, we require at least three microphones for determining a unique AOA solution.

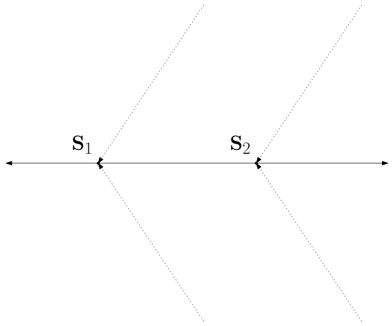

Figure 2. There are two microphones, $\mathbf{S}_1$ and $\mathbf{S}_2$. A straight infinite line connects these two microphones. Dotted arrows indicate the signal direction at each microphone. Utilizing the phase differences at these two microphones, we cannot determine whether the target exists to the left or to the right of this line.

Using (5), we obtain

$$D_2 - D_1 = \frac{\mathbf{S}_2 \cdot \mathbf{u}}{C} - \frac{\mathbf{S}_1 \cdot \mathbf{u}}{C}. \tag{6}$$

Using (1) and Figure 1, we further obtain

$$\frac{D_2 - D_1}{r} = \frac{c(\frac{2\pi}{3})c(\phi) + s(\frac{2\pi}{3})s(\phi)}{C} - \frac{c(\phi)}{C}. \tag{7}$$

Using (5), we have

$$D_2 - D_3 = \frac{\mathbf{S}_2 \cdot \mathbf{u}}{C} - \frac{\mathbf{S}_3 \cdot \mathbf{u}}{C}. \tag{8}$$

Using (1) and Figure 1, we further obtain

$$\frac{D_2 - D_3}{r} = \frac{c(\frac{2\pi}{3})c(\phi) + s(\frac{2\pi}{3})s(\phi)}{C} - \frac{c(\frac{2\pi}{3})c(\phi) - s(\frac{2\pi}{3})s(\phi)}{C}. \tag{9}$$

(7) and (9) lead to

$$\frac{C}{r}(D_2 - D_1, D_2 - D_3)^T = \mathbf{M}(c(\phi), s(\phi))^T, \tag{10}$$

where

$$\mathbf{M} = \begin{pmatrix} c(\frac{2\pi}{3}) - 1 & s(\frac{2\pi}{3}) \\ 0 & 2s(\frac{2\pi}{3}) \end{pmatrix}. \tag{11}$$

Then, (10) leads to

$$\frac{r}{C}(c(\phi), s(\phi))^T = \mathbf{M}^{-1}(D_2 - D_1, D_2 - D_3)^T. \tag{12}$$

Using the fact that $\|(c(\phi), s(\phi))\| = 1$, we estimate $(c(\phi), s(\phi))$ as

$$(c(\phi), s(\phi))^T = \frac{\mathbf{M}^{-1}(D_2 - D_1, D_2 - D_3)^T}{\|\mathbf{M}^{-1}(D_2 - D_1, D_2 - D_3)^T\|}. \tag{13}$$

We then estimate ϕ as

$$\phi = atan2(s(\phi), c(\phi)). \tag{14}$$

Note that we do not have to access either r or C, since $(c(\phi), s(\phi))^T$ is derived using (13). Recall that using the phase at f_i ($i \in \{1, 2, 3\}$), we can compute the signal delay D_i.

It is acknowledged that (13) is singular when $D_1 = D_2 = D_3$. In this case, the signal delay of every microphone is identical to that of any other microphone. In this case, one cannot estimate the bearing angle ϕ under (14). Next, we present the requirement to enable a microphone configuration with three microphones to estimate ϕ.

3.1. AOA Estimator with a General Configuration Composed of Three Microphones

In this subsection, we consider an AOA estimator which has a general microphone configuration with three microphones, which is distinct from Figure 1. This paper considers a general configuration composed of three microphones. A general microphone configuration considered in this subsection is depicted in Figure 3. In this figure, A_j denotes the angle of the j-th microphone measured in the counter-clockwise direction starting from the x-axis of the microphone configuration. Moreover, r_j denotes the distance between the center and the j-th microphone.

Considering a general microphone configuration with three microphones, $r_j \neq r_k$ is feasible, where $j \neq k$. To avoid the phase wrapping case, this paper assumes that $max([r_1, r_2, r_3])$ is less than half of the wavelength.

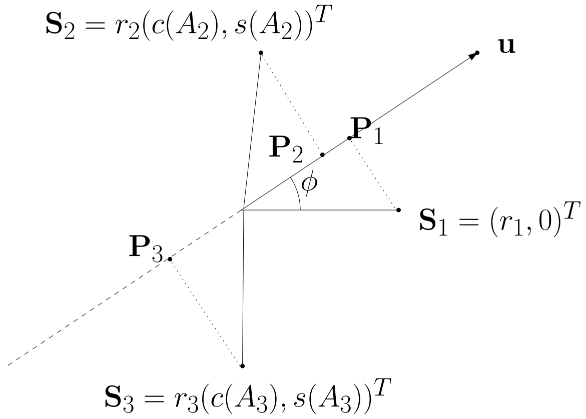

Figure 3. A general configuration with three microphones. $\mathbf{u}$ defines the unit vector from the origin to the target. ϕ defines the bearing angle of the target signal, such that $-\pi < \phi \leq \pi$. $\mathbf{S}_i$ ($i \in \{1, 2, 3\}$) defines the 2D coordinates of the i-th microphone. $\mathbf{P}_i$ defines the projection of $\mathbf{S}_i$ onto $\mathbf{u}$. A_j denotes the angle of the j-th microphone measured in the counter-clockwise direction starting from the x-axis of the microphone configuration. Moreover, r_j denotes the distance between the center and the j-th microphone.

Figure 4 shows a singular microphone configuration where $D_1 = D_2 = D_3$. In this configuration, $\mathbf{P}_1 = \mathbf{P}_2 = \mathbf{P}_3$. Thus, one cannot determine whether the signal direction is $\mathbf{u}$ or $-\mathbf{u}$. Therefore, a microphone configuration with three microphones must satisfy

$$(D_1 - D_2)^2 + (D_2 - D_3)^2 \neq 0. \tag{15}$$

Suppose that (15) is satisfied for a microphone configuration with three microphones. Using (5), we obtain

$$D_2 - D_1 = \frac{\mathbf{S}_2 \cdot \mathbf{u}}{C} - \frac{\mathbf{S}_1 \cdot \mathbf{u}}{C}. \tag{16}$$

Using (1) and Figure 3, we further obtain

$$D_2 - D_1 = \frac{r_2(c(A_2)c(\phi) + s(A_2)s(\phi))}{C} - \frac{r_1 c(\phi)}{C}. \tag{17}$$

Using (5), we have

$$D_2 - D_3 = \frac{\mathbf{S}_2 \cdot \mathbf{u}}{C} - \frac{\mathbf{S}_3 \cdot \mathbf{u}}{C}. \tag{18}$$

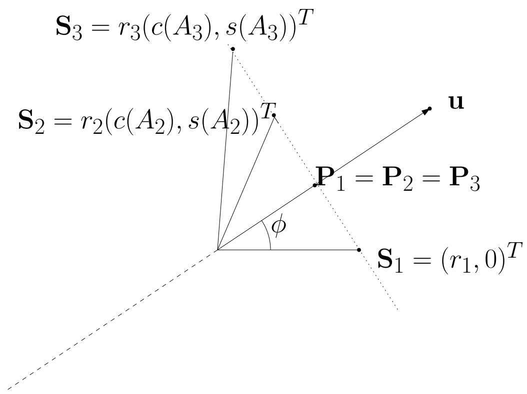

Figure 4. A singular microphone configuration where $D_1 = D_2 = D_3$. $\mathbf{u}$ defines the unit vector from the origin to the target. ϕ defines the bearing angle of the target signal, such that $-\pi < \phi \leq \pi$. $\mathbf{S}_i$ ($i \in \{1,2,3\}$) defines the 2D coordinates of the i-th microphone. $\mathbf{P}_i$ defines the projection of $\mathbf{S}_i$ onto $\mathbf{u}$. A_j denotes the angle of the j-th microphone measured in the counter-clockwise direction starting from the x-axis of the microphone configuration. Moreover, r_j denotes the distance between the center and the j-th microphone. One cannot determine whether the signal direction is $\mathbf{u}$ or $-\mathbf{u}$.

Using (1) and Figure 3, we further obtain

$$D_2 - D_3 = \frac{r_2(c(A_2)c(\phi) + s(A_2)s(\phi))}{C} - \frac{r_3(c(A_3)c(\phi) + s(A_3)s(\phi))}{C}. \tag{19}$$

(17) and (19) lead to

$$C(D_2 - D_1, D_2 - D_3)^T = \mathbf{G}(c(\phi), s(\phi))^T, \tag{20}$$

where

$$\mathbf{G} = \begin{pmatrix} r_2 c(A_2) - r_1 & r_2 s(A_2) \\ r_2 c(A_2) - r_3 c(A_3) & r_2 s(A_2) - r_3 s(A_3) \end{pmatrix}. \tag{21}$$

Then, (20) leads to

$$\frac{1}{C}(c(\phi), s(\phi))^T = \mathbf{G}^{-1}(D_2 - D_1, D_2 - D_3)^T. \tag{22}$$

Using the fact that $\|(c(\phi), s(\phi))\| = 1$, we estimate $(c(\phi), s(\phi))$ as

$$(c(\phi), s(\phi))^T = \frac{\mathbf{G}^{-1}(D_2 - D_1, D_2 - D_3)^T}{\|\mathbf{G}^{-1}(D_2 - D_1, D_2 - D_3)^T\|}. \tag{23}$$

In order to satisfy the existence of $\mathbf{G}^{-1}$, $\mathbf{G}$ must be invertible. For making $\mathbf{G}$ invertible, the condition number of $\mathbf{G}$ must be as close to one as possible. As the condition number of $\mathbf{G}$ increases, $\mathbf{G}$ becomes ill-conditioned. Hence, the condition number of $\mathbf{G}$ in (21) is applied as the observability index of the AOA estimator.

Once the condition number of $\mathbf{G}$ in (21) is less than a certain threshold, *Thres*, and (15) is met, we then estimate ϕ using the proposed AOA estimator (23). Note that we do not have to access either r or C, since $(c(\phi), s(\phi))^T$ is derived using (23). Recall that using the phase at f_i ($i \in \{1,2,3\}$), we can compute the signal delay D_i.

3.2. Computation Load Analysis

In the proposed AOA estimator, FFT is used to find a frequency where the signal amplitude is maximized. The computation load of FFT is $O(N \times logN)$, where N denotes the data size. Reference (14) is used to estimate the target's bearing angle. Once FFT is done, the computation of (14) does not depend on the data size, N. Thus, the computation load of the proposed AOA estimator is $O(N \times logN)$. In the next section, MATLAB simulations show that the proposed AOA estimator outperforms MUSIC estimators considering both computation load and estimation accuracy.

4. MATLAB Simulations

MATLAB simulations (version: MATLAB R2022a) are applied to demonstrate the effectiveness of the proposed AOA estimator with only three microphones. The sampling frequency is $f_s = 500,000$ Hz, and the signal length is set as only 50 samples. Once the condition number of $\mathbf{G}$ in (21) is less than $Thres = 2$ and (15) is met, then we estimate the AOA ϕ using the proposed AOA estimator (23).

Suppose that each microphone measures a real-valued sound signal whose frequency information or speed are not known in advance. The measured signal is a sinusoidal signal with frequency $f = 10,000$ Hz. Note that the signal frequency f is not known in advance, since one considers a non-cooperative target. The signal speed C is 1400 m/s, but C is not known in advance. In underwater environments, sound speed can change according to various environmental effects (e.g., water temperature and salinity) [1]. In the AOA estimation, a wrong signal speed, e.g., $C_w = 1200$ m/s, is used.

Let $sig[n]$ $(n \in 1, 2, ..., 100)$ denote the real-valued signal sampled at sampling index n. As the real-valued signal, we use

$$sig[n] = c(2\pi f n t_s) + G, \tag{24}$$

where $t_s = 1/f_s$ indicates the sampling period. Considering measurement noise, G indicates a Gaussian noise having zero mean and standard deviation $\sigma_G = 0.5$. This implies that the signal-to-noise ratio (SNR) is $10log(\frac{1}{0.5}) = 10log(2)$ in dB.

Recall that the signal delay D_i $(i \in \{1,2,3\})$ was addressed in (5). Then, the signal at each microphone $\mathbf{S}_i$ ($i \in \{1,2,3\}$) is modeled using

$$sig^i[n] = c(2\pi f n t_s + 2\pi f_s D_i) + G. \tag{25}$$

Note that $c(2\pi f n t_s + 2\pi f_s D_i)$ is the real part of a complex-valued exponential number $e^{j2\pi f n t_s} \times e^{j2\pi f_s D_i}$. Since $D_i = \frac{\mathbf{S}_i \cdot \mathbf{u}}{C}$ under (5), we have

$$e^{j2\pi f_s D_i} = e^{j\frac{2\pi f_s}{C}\mathbf{S}_i \cdot \mathbf{u}}. \tag{26}$$

A vector with 3 rows, whose i-th row $(i \in \{1,2,3\})$ is $e^{j2\pi f_s D_i}$ in (26), is termed the *steering* vector in MUSIC estimators [11–13,15].

For robust verification of the proposed estimator using three microphones, we use 100 Monte Carlo (MC) simulations. Recall that ϕ^t denotes the true bearing angle. Let $\hat{\phi}[m]$ denote an estimate of the bearing angle ϕ in the m-th MC simulation ($m \in \{1, 2, ..., 100\}$). Then, we define $avgErr$ (in degrees) as

$$avgErr = \frac{1}{100}\sum_{m=1}^{100}(\hat{\phi}[m] - \phi). \tag{27}$$

We define $stdErr$ (in degrees) as

$$stdErr = \sqrt{\frac{1}{100}\sum_{m=1}^{100}(\hat{\phi}[m]-\phi)^2}. \tag{28}$$

The computation time required for all MC simulation is termed $ComputeTime$ in seconds.

4.1. AOA Estimation Using a Sensor Configuration as Plotted in Figure 1

As the first computer simulation scenario, we use the microphone configuration as plotted in Figure 1. In addition, r, the radius of microphone configuration, is 0.4 of the wavelength. Here, the wavelength, λ, is given as $\lambda = \frac{C}{f}$. See that r is less than half of the wavelength, for removing aliasing in the AOA estimator.

Recall that the condition number of $\mathbf{G}$ in (21) is applied as the observability index of the AOA estimator. For making $\mathbf{G}$ invertible, the condition number of $\mathbf{G}$ must be as close to one as possible. The condition number of $\mathbf{G}$ is 1.73, as we use the microphone configuration in Figure 1. Observe that this condition number is less than $Thres = 2$.

Figure 5 shows the signal strength at every microphone. The target's true bearing angle ϕ is -180 degrees. Under the proposed AOA estimator, we get $avgErr = 0.2$ degrees. In addition, we get $stdErr = 1.3$ degrees. $ComputeTime$ is 0.04 s. Observe that the proposed estimation is accurate and fast.

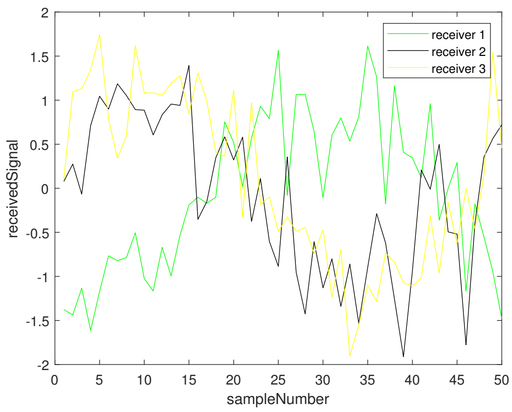

Figure 5. The signal strength at every microphone ($\sigma_G = 0.5$). This implies that the signal-to-noise ratio (SNR) is $10log(\frac{1}{0.5}) = 10log(2)$ in dB.

4.1.1. Change the Target's Bearing Angle

For comparison with the proposed AOA estimator using only three microphones, this study uses the MUSIC estimator [11–13]. Considering the case where only three microphones are used, one shows that the proposed estimator outperforms the MUSIC estimator considering both estimation accuracy and computation time.

The MUSIC estimator [11–13] estimates the autocorrelation matrix utilizing an eigenspace method. In the MUSIC estimator, AOA search is used with step size (0.5 degree) in the range of (-180, -179.5, ..., 179.5, 180) in degrees. One can decrease the step size to improve the estimation accuracy. However, decreasing the step size increases the AOA computation load; thus, there is a trade-off between decreasing the step size and the computation load.

We change the target's bearing angle gradually and test the performance of the proposed AOA estimator (Pro) and the MUSIC estimator (MU). Table 1 depicts the simulation results. Considering measurement noise, (24) uses $\sigma_G = 0.1$. This implies that the signal-to-noise ratio (SNR) is $10log(\frac{1}{0.1}) = 10$ in dB.

The unit for angle measurements in the table is degrees. $ComputeTime$ for all Pro MC simulations in Table 1 is 0.6 s, and $ComputeTime$ for all MU MC simulations in Table 1 is 2 s.

Table 1. Algorithm comparison ($SNR = 10$).

ϕ	$Pro(avgErr)$	$Pro(stdErr)$	$MU(avgErr)$	$MU(stdErr)$
−180	0.04	0.2	−0.01	0.4
−160	−0.02	0.2	−134	0.5
−140	0.03	0.2	134	0.5
−120	0.03	0.2	0.02	0.4
−100	0.04	0.2	−134	0.4
−80	−0.03	0.2	134	0.3
−60	−0.04	0.2	−0.05	0.4
−40	−0.007	0.2	−134	0.3
−20	0.001	0.2	134	0.4
0	−0.004	0.2	−0.05	0.4
20	0.01	0.2	−134	0.3
40	0.009	0.2	134	0.4
60	0.01	0.2	0.02	0.3
80	−0.01	0.2	−134	0.3
100	−0.009	0.2	134	0.3
120	−0.004	0.2	−0.01	0.4
140	0.01	0.2	−134	0.3
160	0.02	0.2	136	0.4

For all angles in Table 1, $min(Pro(avgErr)) = -0.04$ and $max(Pro(avgErr)) = 0.04$. For all angles in Table 1, $min(MU(avgErr)) = -134$ and $max(MU(avgErr)) = 136$. Table 1 shows that the proposed AOA estimator outperforms the MUSIC estimator considering both accuracy and computation time.

4.1.2. Change the Noise Level

We change the noise level σ_G in (24) and test the performance of the proposed AOA estimator. We change the noise level σ_G in (24) to 1. This implies that the signal-to-noise ratio (SNR) is $10log(\frac{1}{1}) = 0$ in dB.

Table 2 depicts the simulation results, as we set SNR as zero. $ComputeTime$ for all Pro simulations in Table 2 is 0.6 s and $ComputeTime$ for all MU simulations in Table 2 is 2 s.

For all angles in Table 2, $min(Pro(avgErr)) = -0.5$ and $max(Pro(avgErr)) = 1.8$. For all angles in Table 2, $min(MU(avgErr)) = -128$ and $max(MU(avgErr)) = 125$. Table 2 shows that the proposed AOA estimator outperforms the MUSIC estimator considering both accuracy and computation time.

Table 2. Algorithm comparison ($SNR = 0$).

ϕ	$Pro(avgErr)$	$Pro(stdErr)$	$MU(avgErr)$	$MU(stdErr)$
−180	0.17	2.5	−0.5	32
−160	0.09	2.5	−121	45
−140	0.1	2.3	115	53
−120	1.8	2.5	−0.1	39
−100	−0.5	2.8	−118	54
−80	0.29	2.5	119	50
−60	0.15	2.6	−6	25
−40	0.4	2.7	−128	53
−20	0.2	2.5	125	57
0	−0.3	2.6	−1	19
20	0.01	2.2	−120	50
40	0.003	2.9	119	60
60	−0.5	2.7	−1	27
80	0.3	2.9	−119	65
100	−0.3	2.6	119	65
120	−0.2	2.9	2	23
140	0.01	2.6	−110	58
160	0.1	2.5	109	61

4.2. AOA Estimation Using a General Configuration with Three Microphones

In this subsection, we consider a general configuration with three microphones. Consider the case where $A_2 = \pi/2$ and $A_3 = -\pi/2$ in Section 3.1. Moreover, we set $r_1 = 0.4\lambda$, $r_2 = r_1/2$, and $r_3 = r_1/3$. For avoiding the phase wrapping case, this paper assumes that $max([r_1, r_2, r_3])$ is less than half of the wavelength.

See Figure 6 for this general configuration. Recall that the condition number of $\mathbf{G}$ in (21) is applied as the observability index of the AOA estimator. For making $\mathbf{G}$ invertible, the condition number of $\mathbf{G}$ must be as close to one as possible. The condition number of $\mathbf{G}$ is 1.76, as we use the microphone configuration in Figure 6. Observe that this condition number is less than $Thres = 2$.

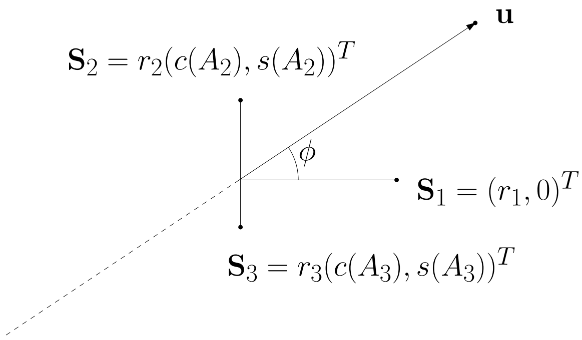

Figure 6. This figure depicts a general microphone configuration. We set $A_2 = \pi/2$ and $A_3 = -\pi/2$ in Section 3.1. Moreover, we set $r_1 = 0.4\lambda$, $r_2 = r_1/2$, and $r_3 = r_1/3$.

The true signal speed C is 1400 m/s, but C is not known in advance. Thus, in each MC simulation, the proposed AOA estimator sets a random number in the interval [0, 1400] as a wrong signal speed C_w.

In this subsection, we change the target's bearing angle gradually and test the performance of the proposed AOA estimator (*General*) with this general microphone configuration. Considering the general microphone configuration, Table 3 depicts the simulation results. Considering measurement noise, (24) uses $\sigma_G = 0.1$. This implies that the signal-to-noise ratio (SNR) is $10log(\frac{1}{0.1}) = 10$ in dB.

The unit for angle measurements in the table is degrees. *ComputeTime* for all *General* MC simulations in Table 3 is 1 s. For all angles in Table 3, $min(General(avgErr)) = -0.08$, and $max(General(avgErr)) = 0.1$. Note that *General* outperforms *MU* in Table 1.

Table 3. Algorithm evaluation ($SNR = 10$).

ϕ	$General(avgErr)$	$General(stdErr)$
−180	0.03	0.5
−160	−0.009	0.5
−140	−0.02	0.5
−120	−0.04	0.4
−100	0.07	0.3
−80	0.04	0.4
−60	−0.04	0.4
−40	0.07	0.4
−20	0.1	0.4
0	0.01	0.4
20	0.07	0.4
40	−0.08	0.4
60	0.05	0.4
80	0.02	0.4
100	−0.06	0.3
120	−0.08	0.5
140	0.1	0.5
160	0.008	0.5

Considering the general microphone configuration with three microphones, Table 4 depicts the simulation results. Considering measurement noise, (24) uses $\sigma_G = 1$. This implies that the signal-to-noise ratio (SNR) is 0. The unit for angle measurements in the table is degrees. $ComputeTime$ for all $General$ MC simulations in Table 4 is 1 s. For all angles in Table 4, $min(General(avgErr)) = -0.9$ and $max(General(avgErr)) = 0.9$. Note that $General$ outperforms MU in Table 2.

Table 4. Algorithm evaluation ($SNR = 0$).

ϕ	$General(avgErr)$	$General(stdErr)$
−180	−0.17	5
−160	−0.04	8
−140	0.9	4
−120	−0.4	4
−100	0.6	3
−80	−0.007	5
−60	0.8	4
−40	0.5	5
−20	−0.7	5
0	0.9	5
20	0.7	9
40	0.2	5
60	0.05	4
80	−0.3	3
100	−0.1	4
120	−0.9	4
140	−0.2	5
160	−0.2	5

4.3. AOA Estimation Using Random Configurations with Three Microphones

In this subsection, we consider random configurations with three microphones. In each MC simulation, we set A_2 in Section 3.1 as a random number in the interval $[-\pi, \pi]$. Also, in each MC simulation, we set A_3 in Section 3.1 as a random number in the interval $[-\pi, \pi]$. We set $r_1 = 0.4\lambda$. In each MC simulation, $r_2 = r_1 * rand$ and $r_3 = r_1 * rand$, where $rand$ returns a random number in the interval $[0, 1]$. In this way, we generate a random microphone configuration at each MC simulation.

For making $\mathbf{G}$ in (21) invertible, the condition number of $\mathbf{G}$ must be as close to one as possible. Thus, in the case where the condition number of $\mathbf{G}$ is less than $Thres = 2$ and (15) is met, the associated MC simulation uses the randomly generated microphone configuration.

The true signal speed C is 1400 m/s, but C is not known in advance. Thus, in each MC simulation, the proposed AOA estimator sets a random number in the interval [0, 1400] as a wrong signal speed C_w.

We change the target's bearing angle gradually and test the performance of the proposed AOA estimator ($Random$) with a randomly generated microphone configuration. Considering a random microphone configuration, Table 5 depicts the simulation results. Considering measurement noise, (24) uses $\sigma_G = 0.1$. This implies that the signal-to-noise ratio (SNR) is $10log(\frac{1}{0.1}) = 10$ in dB.

$ComputeTime$ for all $Random$ MC simulations in Table 5 is 1 s. For all angles in Table 5, $min(Random(avgErr)) = -0.1186$, and $max(Random(avgErr)) = 0.0867$. Note that $Random$ outperforms MU in Table 1.

Next, we check the effect of loosening the requirements for microphone configuration. For making $\mathbf{G}$ invertible, the condition number of $\mathbf{G}$ must be as close to one as possible. In the case where the condition number of $\mathbf{G}$ is less than $Thres = 200$ and (15) is met, the associated MC simulation uses the randomly generated microphone configuration. Using a large $Thres$ implies that we use loose requirements for microphone configuration.

Table 5. Algorithm evaluation ($SNR = 10$)

ϕ	$Random(avgErr)$	$Random(stdErr)$
−180	0.006	0.8
−160	−0.0007	0.6
−140	−0.0731	0.6
−120	0.0428	0.5
−100	−0.0144	0.5
−80	−0.0251	0.4
−60	−0.0552	0.5
−40	−0.0955	0.7
−20	0.0788	0.7
0	0.0713	0.6
20	−0.1147	0.7
40	−0.1186	0.5
60	0.0708	0.5
80	−0.0136	0.4
100	0.0631	0.4
120	0.0867	0.5
140	−0.0250	0.5
160	−0.0391	0.6

$ComputeTime$ for all $Random$ MC simulations in Table 6 is 1 s. For all angles in Table 6, $min(Random(avgErr)) = -1.2953$, and $max(Random(avgErr)) = 0.8627$. Compared to Table 5, the estimation accuracy decreased in Table 6, since the requirements for microphone configuration are loose in Table 6. This shows that the condition number of **G** is suitable for the observability index of the AOA estimator.

Table 6. Algorithm evaluation of loose requirements for microphone configuration ($SNR = 10$)

ϕ	$Random(avgErr)$	$Random(stdErr)$
−180	−0.9335	6
−160	−0.1944	5
−140	−0.4441	5
−120	−0.1736	3
−100	0.0418	1
−80	0.1143	1
−60	−0.3400	4
−40	−0.0172	2
−20	−0.2771	7
0	−0.6291	6
20	−1.2953	7
40	0.8627	3
60	−0.0311	1
80	−0.4495	4
100	−0.2153	1
120	−0.1763	2
140	0.0353	2
160	0.4147	5

5. Discussion

This study handles the case where only a single sound source exists. In practice, there can be multiple signal sources [22–24]. Under the assumption that sound sources rarely overlap in the time-frequency domain, one can apply the proposed AOA scheme for estimating the AOA of every sound source. Thereafter, delay-and-sum beamforming in [25–27] can separate sound arriving from an estimated sound direction.

6. Conclusions

Considering a small underwater platform (e.g., underwater unmanned vehicle), this article addresses how to estimate the signal direction utilizing the minimum number of omnidirectional microphones. Suppose that each omnidirectional microphone measures a real-valued sound signal whose speed and frequency information are not known in advance. This paper addresses how to estimate the AOA of the incoming signal utilizing only three omnidirectional microphones. This study further presents how to estimate the AOA using a general configuration composed of three microphones.

The effectiveness of the proposed AOA estimator with only three omnidirectional microphones is demonstrated by comparing it with the MUSIC algorithm under computer simulations. Considering the case where only three microphones are used, this paper shows that the proposed estimator outperforms the MUSIC estimator considering both estimation accuracy and computation time.

In the future, we will extend the proposed AOA estimator to 3D environments. In 3D environments, one needs more than three omnidirectional microphones to estimate the elevation and azimuth of a 3D non-cooperative target. We will study the minimum number of omnidirectional microphones for estimating the elevation and azimuth of a 3D non-cooperative target.

Funding: This work was supported by the Korea Research Institute for defense Technology planning and advancement (KRIT) grant funded by the Korea government (DAPA (Defense Acquisition Program Administration)) (No. KRIT-CT-22-052, Physics-guided Intelligent Sonar Signal Detection Research Laboratory, 2024)

Institutional Review Board Statement: Not applicable.

Informed Consent Statement: Not applicable.

Data Availability Statement: Data are contained within the article.

Conflicts of Interest: The author declares no conflicts of interest.

References

1. Li, B.; Zhai, J. A Novel Sound Speed Profile Prediction Method Based on the Convolutional Long-Short Term Memory Network. *J. Mar. Sci. Eng.* **2022**, *10*, 572. [CrossRef]
2. Nardone, S.C.; Aidala, V.J. Observability Criteria for Bearings-Only Target Motion Analysis. *IEEE Trans. Aerosp. Electron. Syst.* **1981**, *AES-17*, 162–166. [CrossRef]
3. Fascista, A.; Ciccarese, G.; Coluccia, A.; Ricci, G. Angle of Arrival-Based Cooperative Positioning for Smart Vehicles. *IEEE Trans. Intell. Transp. Syst.* **2018**, *19*, 2880–2892. [CrossRef]
4. Peach, N. Bearings-only tracking using a set of range-parameterised extended Kalman filters. *IEE Proc. Control Theory Appl.* **1995**, *142*, 73–80. [CrossRef]
5. Kim, J. Obstacle Information Aided Target Tracking Algorithms for Angle-Only Tracking of a Highly Maneuverable Target in Three Dimensions. *IET Radar Sonar Navig.* **2019**, *13*, 1074–1080. [CrossRef]
6. Ristic, B.; Arulampalam, M.S. Tracking a manoeuvring target using angle-only measurements: algorithms and performance. *Signal Process.* **2003**, *83*, 1223–1238. [CrossRef]
7. Kim, H.; Kang, K.; Shin, J.W. Factorized MVDR Deep Beamforming for Multi-Channel Speech Enhancement. *IEEE Signal Process. Lett.* **2022**, *29*, 1898–1902. [CrossRef]
8. Yazdi, N.; Todros, K. Measure-Transformed MVDR Beamforming. *IEEE Signal Process. Lett.* **2020**, *27*, 1959–1963. [CrossRef]
9. Ibrahim, E.N.; Khalil, E. Improve the robustness of MVDR beamforming method based on steering vector estimation and sparse constraint. In Proceedings of the 2019 International Symposium on Advanced Electrical and Communication Technologies (ISAECT), Rome, Italy, 27–29 November 2019 ; pp. 1–5.
10. Li, W.; Tang, Q.; Huang, C. A New Close Form Location Algorithm with AOA and TDOA for Mobile User. *Wirel. Pers. Commun.* **2017**, *97*, 3061–3080. [CrossRef]
11. Tota, R.; Hossain, M.S. Three Dimentional Multiple Near-field Source Localization Based on MUSIC Algorithm to Increase the Localization Accuracy of Optimal Beamformer. In Proceedings of the 2021 3rd International Conference on Electrical & Electronic Engineering (ICEEE), Rajshahi, Bangladesh, 22–24 December 2021; pp. 9–12.
12. Santos, E.; Zoltowski, M. Spatial power spectrum estimation based on a MVDR-MMSE-MUSIC hybrid beamformer. In Proceedings of the Proceedings. (ICASSP '05). IEEE International Conference on Acoustics, Speech, and Signal Processing, 2005, Philadelphia, PA, USA, 23–23 March 2005; Volume 4, pp. iv/809–iv/812.

13. Ahmed, I.; Anirudh Koushik, B.; Charan Kumar, G.; Neethu, S. Simulation of Direction of Arrival Using MUSIC Algorithm and Beamforming using Variable Step Size LMS Algorithm. In Proceedings of the 2022 IEEE Microwaves, Antennas, and Propagation Conference (MAPCON), Bangalore, India, 12–16 December 2022; pp. 993–997.
14. Lei, S.; Wu, Y.; Wang, X.; Wang, Z.; Yang, S. Adaptive Beamformer Based on Effectiveness of Reconstruction. In Proceedings of the 2019 IEEE 2nd International Conference on Electronic Information and Communication Technology (ICEICT), Harbin, China, 20–22 January 2019; pp. 353–357.
15. Adhikari, K.; Drozdenko, B. Symmetry-Imposed Rectangular Coprime and Nested Arrays for Direction of Arrival Estimation With Multiple Signal Classification. *IEEE Access* **2019**, *7*, 153217–153229. [CrossRef]
16. Zhou, X.; Zhu, F.; Jiang, Y.; Zhou, X.; Tan, W.; Huang, M. The Simulation Analysis of DOA Estimation Based on MUSIC Algorithm. In Proceedings of the 2020 5th International Conference on Mechanical, Control and Computer Engineering (ICMCCE), Harbin, China, 25–27 December 2020; pp. 1483–1486.
17. Wen, F.; Javed, U.; Yang, Y.; He, D.; Zhang, Y. Improved subspace direction-of-arrival estimation in unknown nonuniform noise fields. In Proceedings of the 2016 Fourth International Conference on Ubiquitous Positioning, Indoor Navigation and Location Based Services (UPINLBS), Shanghai, China, 2–4 November 2016; pp. 230–233.
18. Mao, Z.; Li, B.; Dong, L.; Qiao, Y.; Sun, H.; Li, Y. An Effective Algorithm for Direction-of-Arrival Estimation of Coherent Signals with ULA. In Proceedings of the 2023 5th International Conference on Natural Language Processing (ICNLP), Guangzhou, China, 24–26 March 2023; pp. 136–140.
19. Lin, B.; Hu, G.; Zhou, H.; Zheng, G.; Song, Y. The DOA Estimation Method for Low-Altitude Targets under the Background of Impulse Noise. *Sensors* **2022**, *22*, 4853. [CrossRef] [PubMed]
20. Kintz, A.L.; Gupta, I.J. A Modified MUSIC Algorithm for Direction of Arrival Estimation in the Presence of Antenna Array Manifold Mismatch. *IEEE Trans. Antennas Propag.* **2016**, *64*, 4836–4847. [CrossRef]
21. Mohanna, M.; Rabeh, M.L.; Zieur, E.M.; Hekala, S. Optimization of MUSIC algorithm for angle of arrival estimation in wireless communications. *NRIAG J. Astron. Geophys.* **2013**, *2*, 116–124. [CrossRef]
22. Florio, A.; Avitabile, G.; Coviello, G. Multiple Source Angle of Arrival Estimation Through Phase Interferometry. *IEEE Trans. Circuits Syst. II Express Briefs* **2022**, *69*, 674–678. [CrossRef]
23. Cai, X.; Sarabandi, K. A Fast Analytic Multiple-Sources Angle-of-Arrival Estimation Algorithm for Automotive MIMO Radars. In Proceedings of the 2020 IEEE International Symposium on Antennas and Propagation and North American Radio Science Meeting, Montreal, QC, Canada, 5–10 July 2020; pp. 1301–1302.
24. Cobos, M.; Lopez, J.J.; Spors, S. A sparsity-based approach to 3D binaural sound synthesis using time-frequency array processing. *EURASIP J. Adv. Signal Process* **2010**, *2010*, 415840. [CrossRef]
25. Xia, H.; Ma, Y.; Yang, K.; Cao, R.; Chen, P.; Li, H. Delay-and-sum beamforming based on the diagonal reducing method. In Proceedings of the OCEANS 2017—Aberdeen, Aberdeen, UK, 19–22 June 2017; pp. 1–5.
26. Van Veen, B.; Buckley, K. Beamforming: A versatile approach to spatial filtering. *IEEE ASSP Mag.* **1988**, *5*, 4–24. [CrossRef] [PubMed]
27. Hussain, A.; Chellappan, K.; Zamratol M., S. Evaluation of multichannel speech signal separation with beamforming techniques. In Proceedings of the 2014 IEEE Conference on Biomedical Engineering and Sciences (IECBES), Kuala Lumpur, Malaysia, 8–10 December 2014; pp. 766–771.